1 Comparison of Hierarchical Posterior to Observations

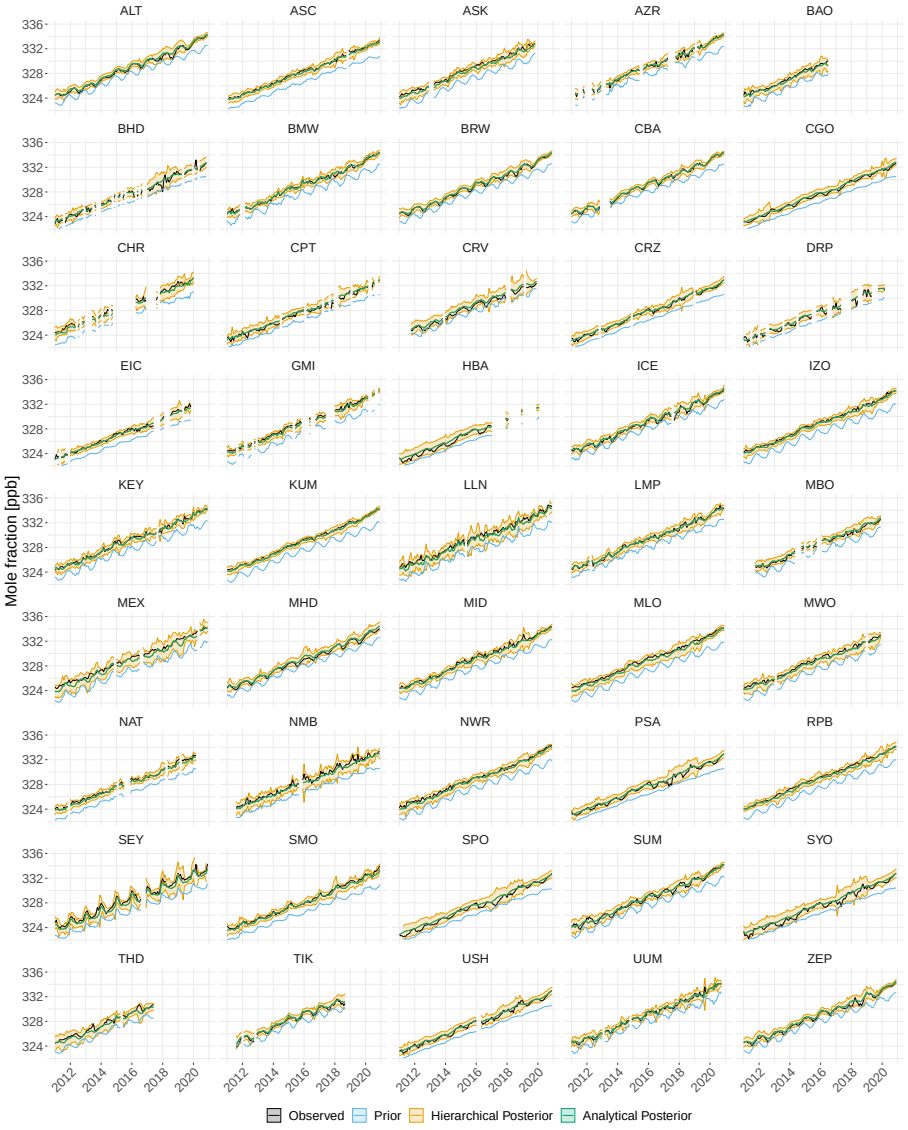

Figure S1: A comparison of the mole fraction generated with the posterior fluxes for the hierarchical (green) and analytical (orange) inversions to the observations (black) and the mole fraction generated with the prior emissions (blue). The shading shows the 95 % credible intervals for the hierarchical inversion posterior. Each panel is titled by a three letter code corresponding to the observation stations listed in Table 1 of the main text of the paper.

Table S1: The median difference (MD) (modelled - observed) between the GEOS-Chem simulation and the observations used in the inversion.

	Median difference to observations / ppb
Prior	-1.494
Hierarchical Posterior	-0.012
Analytical Posterior	-0.021

2 Validation against HIPPO

In order to validate the inversion results, a GEOS-Chem simulation with the posterior fluxes from the hierarchical inversion was run. The output from this run was compared to the HIAPER Pole-to-Pole Observations (HIPPO) aircraft data, which was not used to optimise the fluxes in the inversion. The results of this comparison is shown in Fig. S2 and Fig. S3, for HIPPO IV (14 June to 11 July, 2011) and HIPPO V (9 August to 8 September, 2011), respectively. The posterior fluxes are a much better match to the observations than the prior fluxes, which is additionally demonstrated by the median difference shown in Table S2.

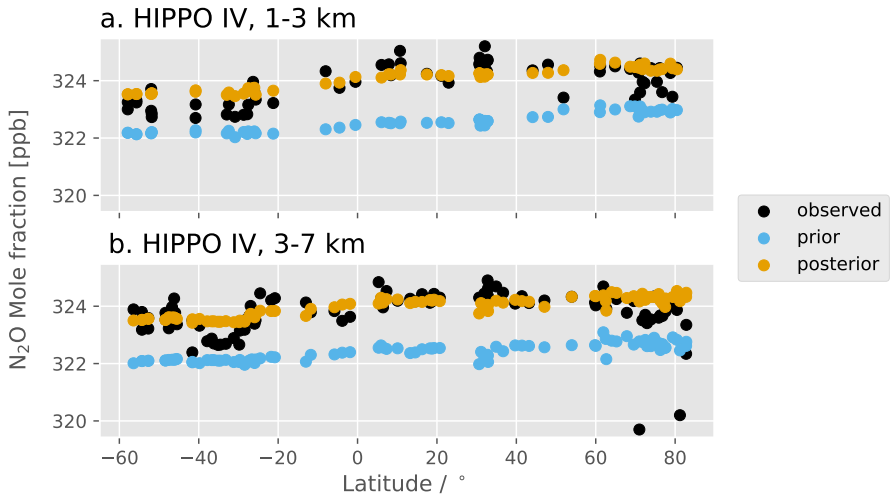

Figure S2: Comparison of the nitrous oxide mole fraction observed in the HIPPO IV campaign (red points) and that simulated in the inversion (blue points are the prior and purple points are the posterior). The data has been split into two groups: a. measurements between 1 and 3 km altitude, and b. measurements between 3 and 7 km altitude.

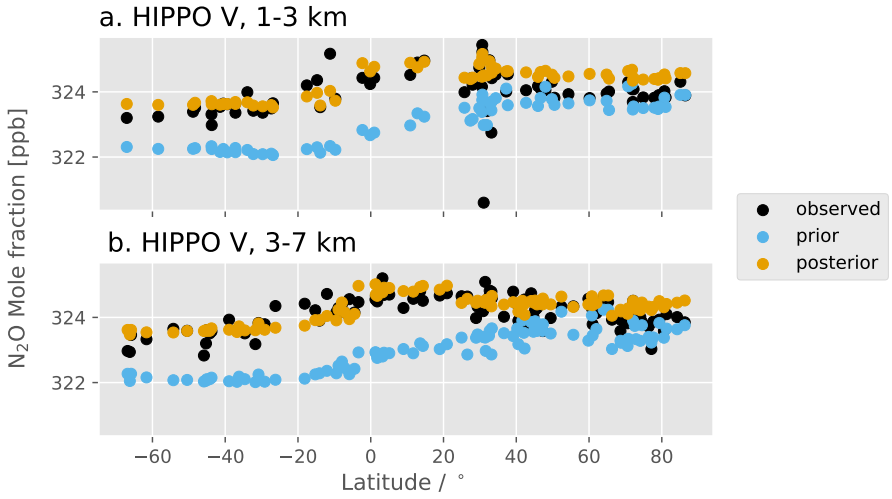

Figure S3: Comparison of the nitrous oxide mole fraction observed in the HIPPO V campaign (red points) and that simulated in the inversion (blue points are the prior and purple points are the posterior). The data has been split into two groups: a. measurements between 1 and 3 km altitude, and b. measurements between 3 and 7 km altitude.

Table S2: The median difference (MD) (modelled - observed) between the GEOS-Chem simulation and the observations for the HIPPO IV and HIPPO V flights.

Campaign	Prior MD / ppb	Posterior MD / ppb
HIPPO IV	-1.49	0.10
HIPPO V	-1.14	0.21

3 Regional Emissions

The TransCom regions used in this work are shown in Fig. S4. The inferred nitrous oxide emissions in each of these regions is presented in this section, with the note that they may be unreliable estimates, as discussed in the main text of the paper.

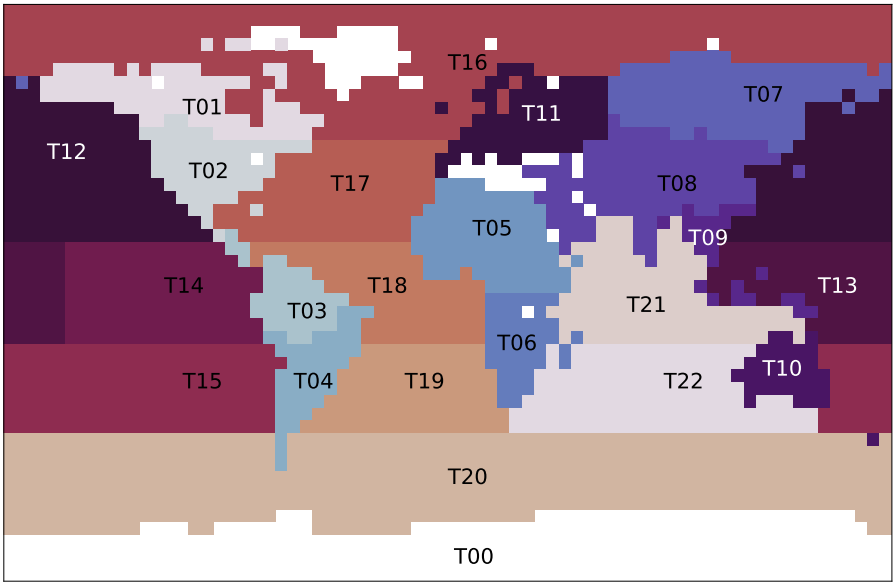

Figure S4: A map of the 23 TransCom regions used in this work.

3.1 Land Regions

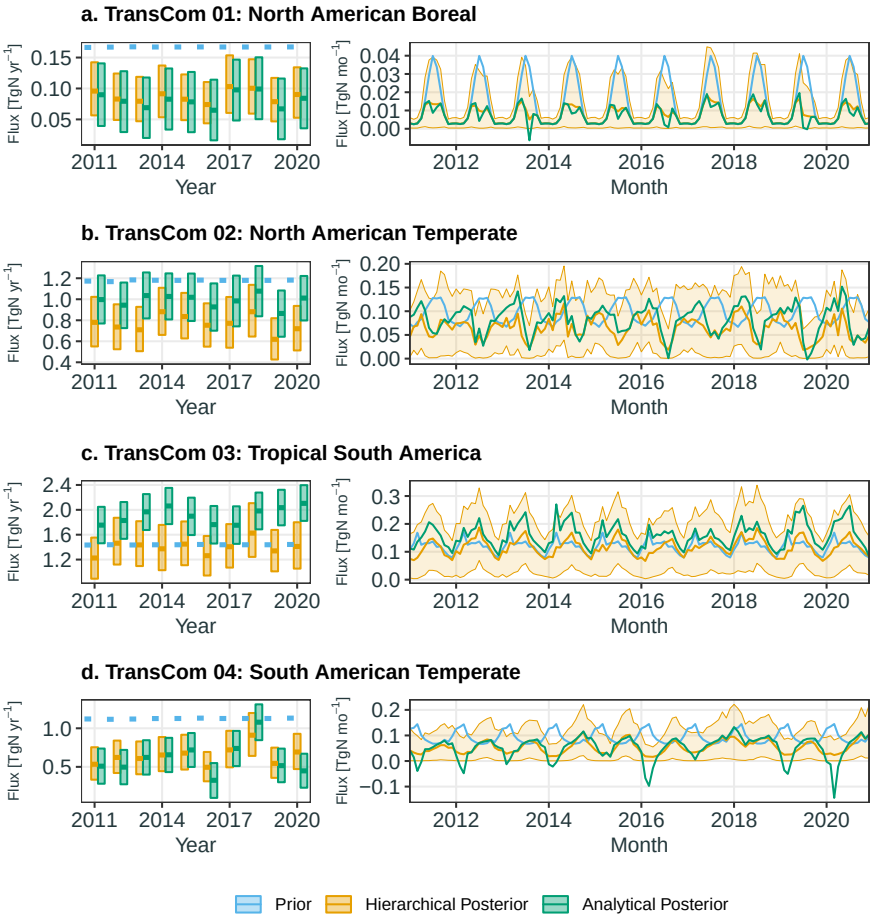

Figure S5: The inferred nitrous oxide emissions for 2011-2020 in four TransCom regions: a. North American Boreal, b. North American Temperate, c. Tropical South America, and d. South American Temperate. The left hand side plots show the annually inferred emissions and the right hand side shows the monthly inferred emissions, where the orange is the hierarchical inversion posterior, the green is the analytical inversion posterior, and the blue is the prior, with the shading showing the 95 % credible intervals of the inversion posterior.

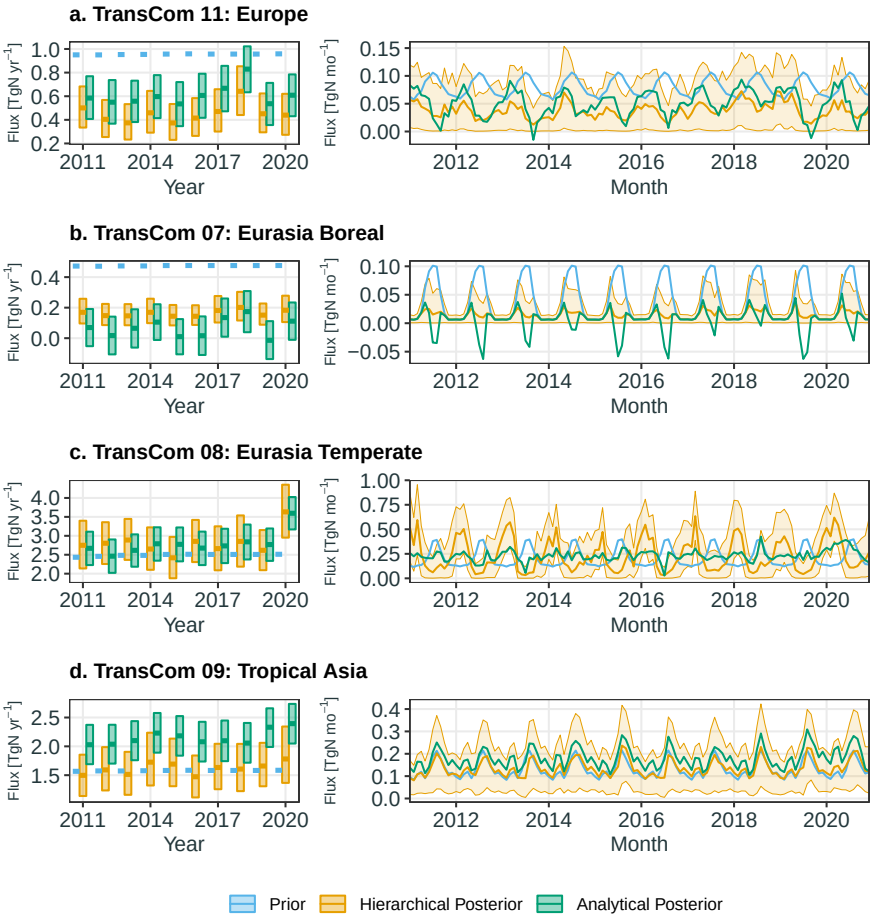

Figure S6: The inferred nitrous oxide emissions for 2011-2020 in four TransCom regions: a. Europe, b. Eurasia Boreal, c. Eurasia Temperate, and d. Tropical Asia. The left hand side plots show the annually inferred emissions and the right hand side shows the monthly inferred emissions, where the orange is the hierarchical inversion posterior, the green is the analytical inversion posterior, and the blue is the prior, with the shading showing the 95 % credible intervals of the inversion posterior.

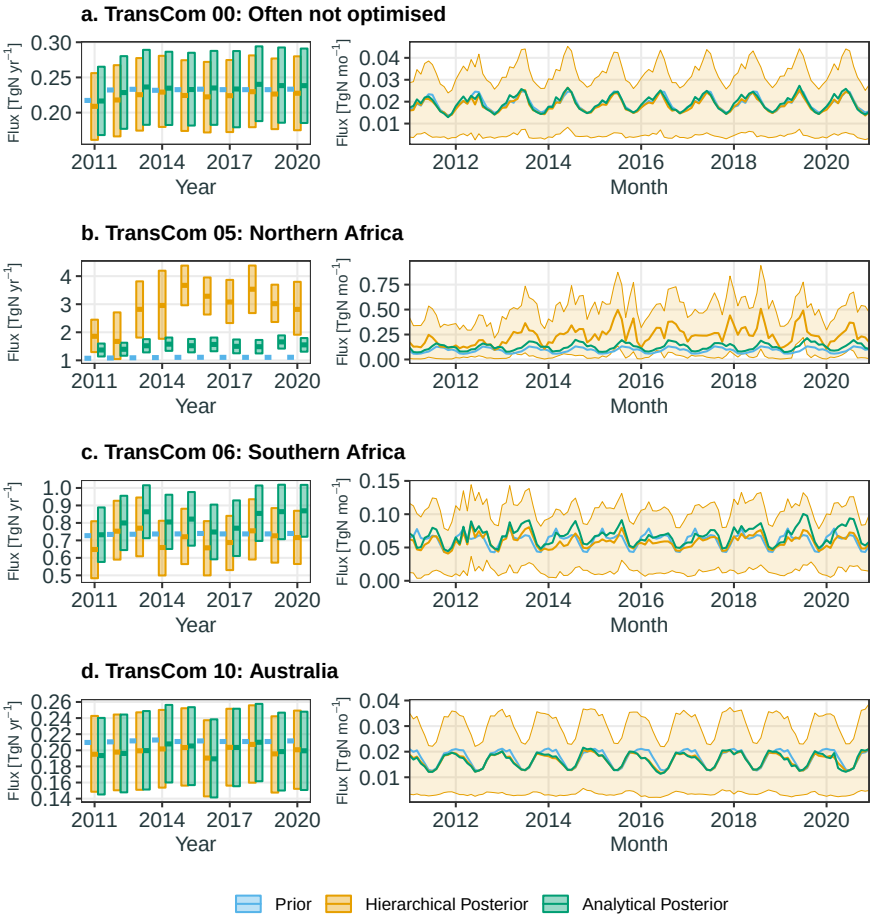

Figure S7: The inferred nitrous oxide emissions for 2011-2020 in four TransCom regions: a. leftover areas such as Antarctica, Greenland, and the Mediterranean Sea, b. Northern Africa, c. Southern Africa, and d. Australia. The left hand side plots show the annually inferred emissions and the right hand side shows the monthly inferred emissions, where the orange is the hierarchical inversion posterior, the green is the analytical inversion posterior, and the blue is the prior, with the shading showing the 95 % credible intervals of the inversion posterior.

3.2 Ocean Regions

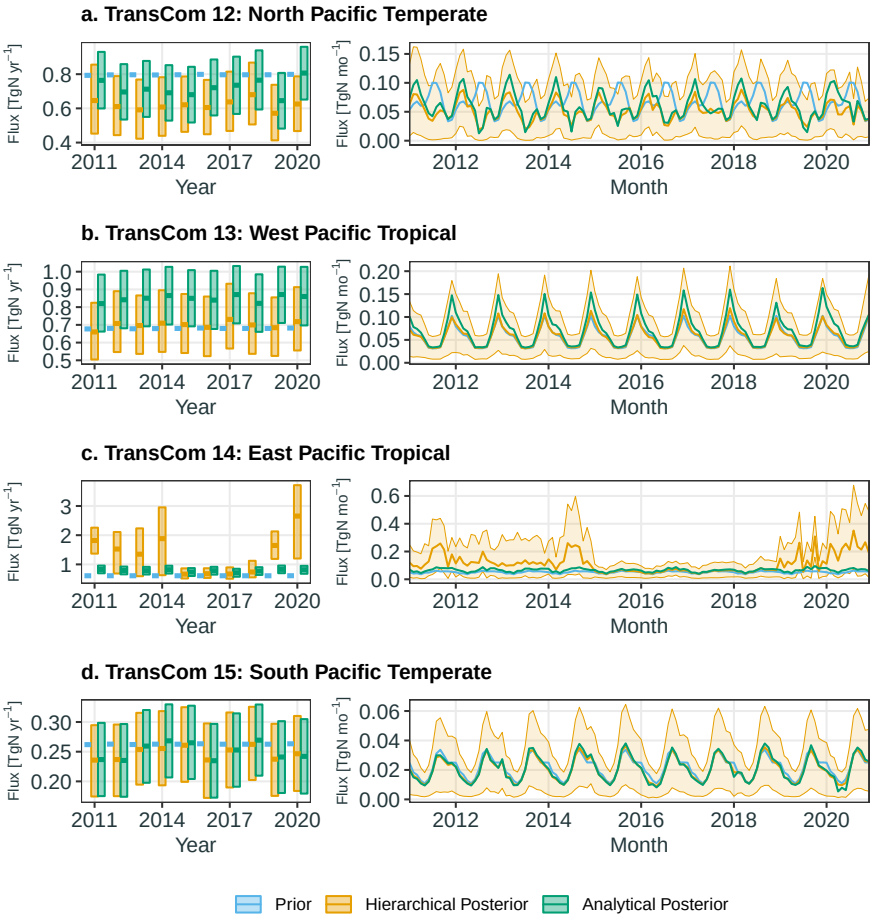

Figure S8: The inferred nitrous oxide emissions for 2011-2020 in four TransCom regions: a. North Pacific Temperate, b. West Pacific Tropical, c. East Pacific Tropical, and d. South Pacific Temperate. The left hand side plots show the annually inferred emissions and the right hand side shows the monthly inferred emissions, where the orange is the hierarchical inversion posterior, the green is the analytical inversion posterior, and the blue is the prior, with the shading showing the 95 % credible intervals of the inversion posterior.

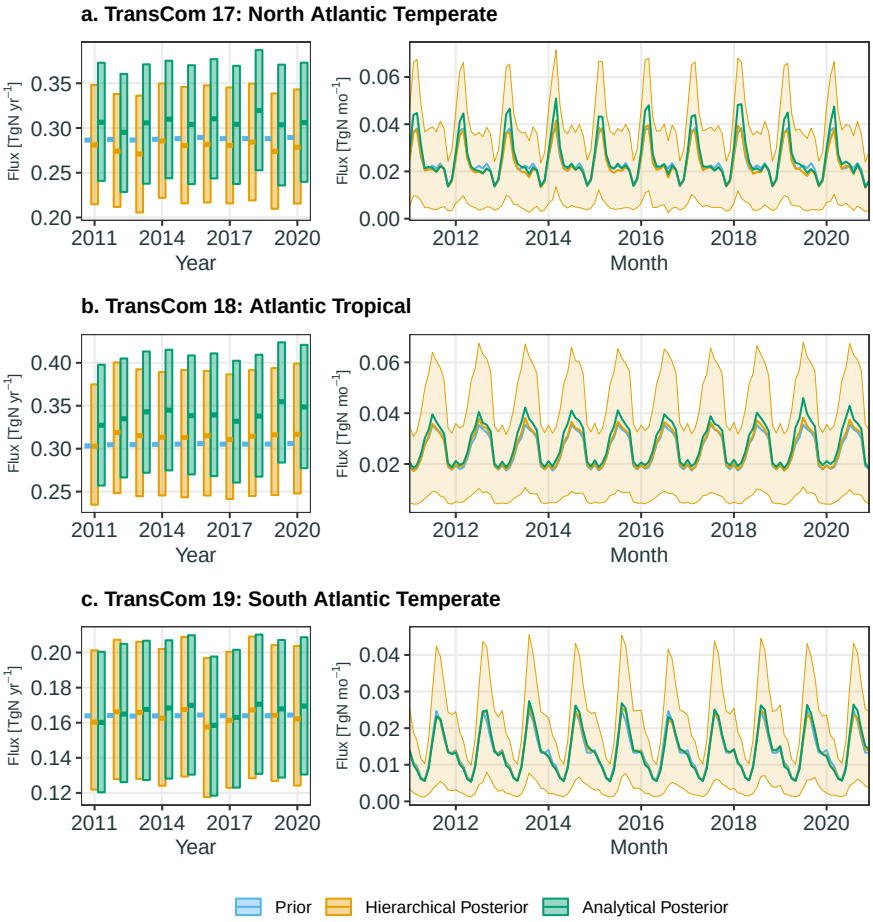

Figure S9: The inferred nitrous oxide emissions for 2011-2020 in three TransCom regions: a. North Atlantic Temperate, b. Atlantic Tropical, and c. South Atlantic Temperate. The left hand side plots show the annually inferred emissions and the right hand side shows the monthly inferred emissions, where the orange is the hierarchical inversion posterior, the green is the analytical inversion posterior, and the blue is the prior, with the shading showing the 95 % credible intervals of the inversion posterior.

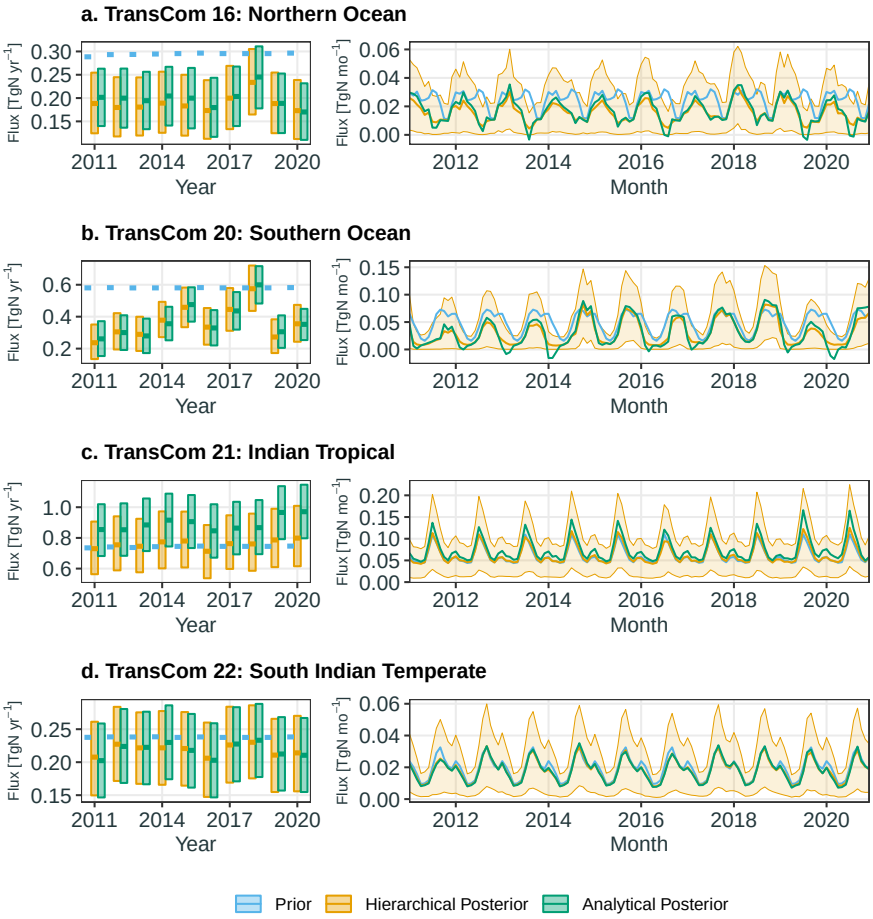

Figure S10: The inferred nitrous oxide emissions for 2011-2020 in four TransCom regions: a. Northern Ocean, b. Southern Ocean, c. Indian Tropical, and d. South Indian Temperate. The left hand side plots show the annually inferred emissions and the right hand side shows the monthly inferred emissions, where the orange is the hierarchical inversion posterior, the green is the analytical inversion posterior, and the blue is the prior, with the shading showing the 95 % credible intervals of the inversion posterior.

4 Hyper-parameter variability

Table S3: The mean of each of the w hyper-parameters over all the years (2011-2020), along with the standard deviation in the mean.

Region	Mean	Standard deviation
TransCom 00: Often not optimised	7.17	0.13
TransCom 01: North American Boreal	3.48	0.13
TransCom 02: North American Temperate	3.24	0.30
TransCom 03: Tropical South America	5.17	0.35
TransCom 04: South American Temperate	2.65	0.20
TransCom 05: Northern Africa	0.38	0.57
TransCom 06: Southern Africa	6.41	0.33
TransCom 07: Eurasia Boreal	2.67	0.10
TransCom 08: Eurasia Temperate	0.46	0.12
TransCom 09: Tropical Asia	5.74	0.34
TransCom 10: Australia	6.76	0.10
TransCom 11: Europe	2.76	0.15
TransCom 12: North Pacific Temperate	3.75	0.60
TransCom 13: West Pacific Tropical	6.69	0.17
TransCom 14: East Pacific Tropical	2.55	2.58
TransCom 15: South Pacific Temperate	6.52	0.17
TransCom 16: Northern Ocean	3.51	0.11
TransCom 17: North Atlantic Temperate	7.10	0.17
TransCom 18: Atlantic Tropical	6.86	0.10
TransCom 19: South Atlantic Temperate	6.92	0.14
TransCom 20: Southern Ocean	2.93	0.77
TransCom 21: Indian Tropical	6.75	0.20
TransCom 22: South Indian Temperate	6.60	0.14

Table S4: The mean of each of the γ hyper-parameters over all the years (2011-2020), along with the standard deviation in the mean.

Station	Mean	Standard deviation
ALT	1.23	0.15
ASC	1.81	0.27
ASK	0.93	0.18
AZR	1.35	0.38
BAO	1.51	0.47
BHD	0.61	0.26
BMW	1.92	0.33
BRW	1.43	0.18
CBA	1.95	0.36
CGO	0.68	0.20
CHR	0.79	0.21
CPT	0.90	0.11
CRV	0.56	0.06
CRZ	1.10	0.36
DRP	0.54	0.09
EIC	1.11	0.43
GMI	1.12	0.25
HBA	0.57	0.18
ICE	1.19	0.12
IZO	1.35	0.28
KEY	1.88	0.16
KUM	1.97	0.32
LLN	0.84	0.19
LMP	2.02	0.14
MBO	1.25	0.25
MEX	0.42	0.07
MHD	0.82	0.22
MID	1.17	0.21
MLO	0.72	0.18
MWO	1.81	0.28
NAT	1.55	0.44
NMB	1.14	0.14
NWR	1.41	0.64
PSA	0.72	0.21
RPB	0.81	0.27
SEY	0.79	0.18
SMO	1.38	0.48
SPO	0.51	0.18
SUM	0.83	0.22
SYO	0.44	0.16
THD	1.01	0.16
TIK	1.20	0.41
USH	0.76	0.17
UUM	1.80	0.21
ZEP	1.21	0.22